



Physicochemical and supercapacitive properties of electroplated nickel oxide electrode: effect of solution molarity

I. A. Dhole^{1,2} · Y. H. Navale¹ · C. S. Pawar² · S. T. Navale³ · V. B. Patil¹

Received: 15 August 2017 / Accepted: 5 January 2018 / Published online: 17 January 2018
© Springer Science+Business Media, LLC, part of Springer Nature 2018

Abstract

With an aim of physicochemical characteristics and electrochemical supercapacitor studies with X-ray diffraction (XRD), scanning electron microscopy (SEM), energy dispersive X-ray (EDAX) technique, X-ray photoelectron spectroscopy (XPS) and surface wettability, nickel oxide (NiO) thin films of different molarities i.e. (0.1, 0.2, 0.3 and 0.4 M) have been synthesized onto stainless-steel substrate using potentiostatic mode of electrochemical method. The XRD result confirms crystalline nature with cubic crystal structure of the NiO. The SEM micrographs reveal homogenous and smooth surfaces. Existence of Ni and O in EDAX spectrums of all samples supports the formation of NiO. Expected peaks are confirmed from XPS surface analyses. Contact angle measurement of 0.1, 0.2 M film showed hydrophilic, however 0.3, 0.4 M film showed hydrophobic in character. The optimal potential for potentiostatic mode of electrochemical method of NiO is 1.8 V. The electrochemical properties of the NiO electrodes are studied in detail by cyclic voltammogram, galvanostatic charge–discharge and electrochemical impedance spectroscopy measurements. The specific capacitance of the NiO electrode is 667.24 Fg^{-1} in Na_2SO_4 electrolyte of 1 mol/L. The achieved specific energy, power and coulombic efficiency of NiO electrode were 2.55 Whkg^{-1} , 6.23 kWkg^{-1} and 92.86% respectively. Moreover, the NiO electrode shows excellent cyclic performance after 1000 cycles. An effective and convenient technique has been developed to produce nickel oxide material promising for designing of innovative capacitors.

1 Introduction

The world is now facing drop in the accessibility of fossil fuel, environment transform and global warming issues. To solve these crucial problems, there is considerable attention on the improvement of advanced energy storages like supercapacitors, batteries and also on alternative energy sources [1, 2]. Generally, supercapacitors have developed considerable interests due to their higher

energy density and higher power density than conventional capacitors. Low cost, harmless, low internal resistance, fast charge–discharge rates and longer cycle life are few additional merits of the supercapacitors [2, 3] which are classified into two characteristic parts according to mechanisms of charge storages (i) electrochemical double-layer capacitors (EDLCs), and (ii) pseudocapacitors (PCs). In EDLCs, carbon-based materials are broadly utilized for instance, carbon nanofibers, multi walled carbon nanotubes, graphene and activated carbon etc. [4, 5]. In PCs, several types of conducting polymers and nanostructured metal oxides and their composites are frequently used pseudocapacitance is the electrochemical storage of electricity in an electrochemical capacitor [6, 7]. The performance of supercapacitors i.e. specific capacitance (SC), specific energy (E) and cyclic stability mainly depends on the electrode materials in terms of surface area, size and porosity etc. Among nanostructured transition metal oxides, ruthenium oxide (RuO_2) is one of the widely studied electrode materials in pseudocapacitor studies. This is due to its high specific capacitance value and good charge–discharge features [8, 9]. Alternatively, its toxic

✉ V. B. Patil
drvbpatil@gmail.com

¹ Functional Materials Research Laboratory, School of Physical Sciences, Solapur University, Solapur, MS 413255, India

² Material Science Research Laboratory, Department of Physics, Shankarrao Mohite Mahavidyalaya, Akhuj, MS 413101, India

³ Nanshan District Key Lab for Biopolymers and Safety Evaluation, College of Materials Science and Engineering, Shenzhen University, Shenzhen, Guangdong, People's Republic of China

nature and high cost limit the commercialization of RuO₂ potential. Therefore, it is essential to build up alternative materials such as NiO, MnO₂ and Fe₂O₃ etc., to be considered as feasible contenders for high performance supercapacitors [10–12]. Among these different metal oxides, NiO is a suitable material for supercapacitor studies owing to its high theoretical specific capacitance (2573 Fg⁻¹), low-cost, high chemical/thermal stability and environmental friendly nature [13, 14]. Because of its fast redox reactions nanostructured NiO is a significant technical material of interest. Electrochemical performances of nanostructured NiO are considerably dissimilar with respect to its microstructures for example nano/microspheres and nano/micro films [15–17]. This is due to the presence of dissimilarities in the speed of ion shift throughout the charge storage progression about structural morphologies [18]. There are numerous techniques to synthesize NiO for instance, calcination, sol–gel, thermal decomposition and electrodeposition [19–22]. For the synthesis of NiO films, chemical methods are being commonly used rather than physical methods, because they have superior control on growth process and kinetics involved. Chemical methods have advantages like cost-effectiveness, non-hazardousness, reproducibility, simplicity etc., over physical methods. Electrodeposition (ED) is one of the easiest and economical chemical methods with uniform product quality. The basic operation principle of electrodeposition is when electric current is passed throughout a metal salt solution; the metal is deposited at the cathode. Basically, ED can be done by three different ways; i.e. potentiostatic (at constant voltage), galvanostatic (at constant current) and potentiodynamic (potential and current variables

with time). Crystal structure, surface interior and hence the supercapacitive possessions of deposited materials are depending upon these three different types. Analysis of the development of environment friendly low cost supercapacitors with cheaper materials is really important for the development of green energy technology [23–28].

In this work, we report preparation of nickel hydroxide (Ni(OH)₂) of different molarities onto stainless-steel (SS) substrate by potentiostatic electrochemical technique (which is well controllable and relatively inexpensive method) from nickel acetate aqueous solution at room temperature without any catalyst or template. The Ni(OH)₂ electrodes of different molarities were annealed at optimized 500 °C temperature in air which results into the formation of nanostructured bluish NiO electrodes. The obtained films of NiO were characterized by X-ray diffraction (XRD), scanning electron microscopy (SEM), energy dispersive X-ray (EDAX), X-ray photoelectron spectroscopy (XPS) and contact angle measurements (CA). Electrochemical capacitive performances of the NiO electrodes were broadly studied using cyclic voltammogram (CV), galvanostatic charge–discharge measurement and electrochemical impedance spectroscopy (EIS) measurements in Na₂SO₄, NaOH and KOH aqueous electrolyte solutions. A maximum specific capacitance of 667.24 Fg⁻¹ was achieved suggesting that the 0.1 M nanostructured NiO film is a promising electrode material for electrochemical supercapacitors in 1 M aqueous Na₂SO₄ solution of electrolyte. As far as literature survey concerned similar kind of work has not been carried out previously i.e. (by potentiostatic electrochemical deposition). The obtained results are better than the value reported in Table 1, where synthesis of NiO was carried out by using various methods

Table 1 Survey of specific capacitance of NiO electrode with different deposition methods

Sr. No.	Morphology	Synthesis method	Electrolyte	Specific capacitance (Fg ⁻¹)	References
1	NiO nanowall	Hydrothermal	1 M KOH	270	[29]
2	NiO mesoporous	Calcination	2 M KOH	120	[30]
3	Hollow NiO nanofibers	Electrospin	6 M KOH	336	[31]
4	NiO porous	Chemical bath deposition	1 M NaOH	129.5	[32]
			1 M KOH	69.8	
5	NiO hollow nanospheres	Microwave assisted	2 M KOH	585	[33]
6	NiO nanosheet hollow spheres	Low-temperature solution route	2 M KOH	415	[34]
7	NiO nanocrystalline	Chemical bath deposition	2 M KOH	167	[35]
8	Porous NiO	Electrodeposition	1 M KOH	351	[36]
9	Capsule-like NiO nanoparticles	Cathodic electrodeposition	1 M KOH	307.2	[37]
10	Nanostructured NiO	Sonochemical method	1 M KOH	449	[38]
11	NiO	Electrodeposition	1 M KOH	167.3	[39]
12	NiO nanoflake	Electrodeposition	1 M KOH	222	[40]
13	Nanoplatelets NiO	Electrophoretic deposition	0.5 KOH	138	[41]
14	NiO nanoplatelets	Potentiostatic electrodeposition	1 M Na ₂ SO ₄	667.24	Present work

[29–41]. The value obtained in the present case is higher, which possibly due to the nanoplate-like structure of NiO film electrode.

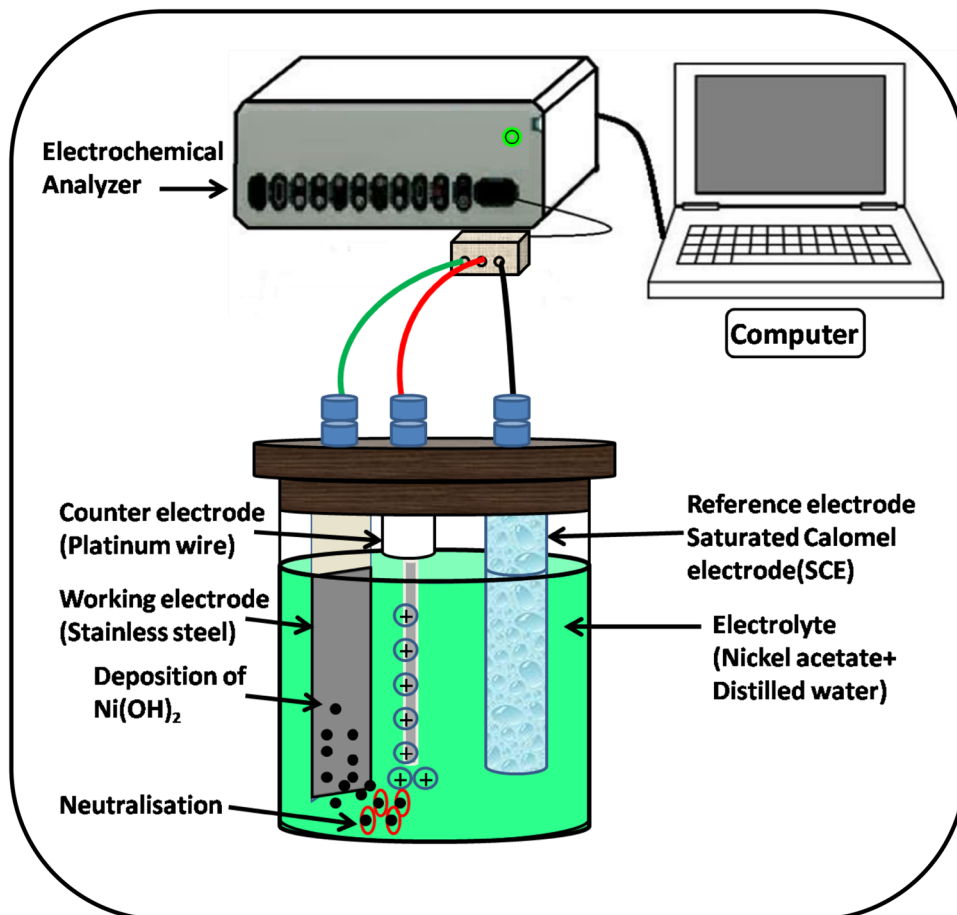
2 Experimental details

Potentiostatic electrochemical deposition technique was used to deposit Ni(OH)₂ films onto SS substrate. The pieces of SS substrate were polished before deposition with polish paper which removes emery particles with rough finishing when dried to air. For synthesis of Ni(OH)₂ films, aqueous solution having different molarities (0.1, 0.2, 0.3 and 0.4 M) of nickel(II) acetate tetra hydrate C₄H₆NiO₄·4H₂O (AR grade) were mixed with distilled water and stirred for 10 min using magnetic stirrer. This stirred solution (electrolyte) was then utilized to deposit Ni(OH)₂ films using a potentiostatic mode. +1.8 V is the deposition voltage which was kept vs. saturated calomel electrode (SCE) which determined from polarization (I–V) curves. The electrochemical deposition of Ni(OH)₂ was carried in a usual three-electrode aqueous bath, containing platinum wire, stainless steel substrate and saturated

calomel electrode as counter electrode, working electrode and reference electrode respectively, which is exposed in Fig. 1. Well-adherent and uniform gray colored films of Ni(OH)₂ were synthesized at room temperature after 60 min. The as-prepared Ni(OH)₂ films were thermally oxidized in tubular furnace at 500 °C temperature in an ambient air for 1 h to obtain NiO films. The synthesized NiO films with four different solution molarities i.e. 0.1, 0.2, 0.3 and 0.4 M were called as N1, N2, N3 and N4, respectively.

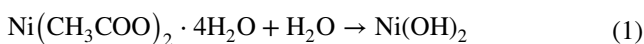
The masses of deposited materials were estimated from the gravimetric weight difference method via sensitive microbalance. ‘*t*’ (thickness of the film) was evaluated by $t = \Delta m / (\rho \times A)$ relation. Here, ‘ Δm ’ (deposited film mass), ‘ ρ ’ (deposited material density) i.e. NiO which is 6.67 g/cm³ and ‘*A*’ (deposited film area). Films obtained N1, N2, N3 and N4 have demonstrated thicknesses of 0.225, 0.398, 0.563 and 0.685 μm , respectively. As the electrolyte concentration (molarity) is enhanced, the deposited mass also enhanced able to certain value and again it is lessen which is revealed in Fig. 3b. This perhaps attributed to the development of tensile stress that tends to a reason delamination while film turn into bulky [42].

Fig. 1 Schematic of formation of Ni(OH)₂ electrode



3 Results and discussion

Figure 2 shows the photo-images of films with different molarities (0.1, 0.2, 0.3 and 0.4 M) of NiO. Greenwood and Earnshaw in 1984 reported that the accurate stoichiometric NiO thin films are likely to have green color; 0.1, 0.2, 0.3 and 0.4 M NiO thin films deposited in the current study are green, greenish, black and blueish in colour respectively, which can be credited to the stoichiometric (0.1, 0.2 and 0.3 M) to nonstoichiometric (0.4 M) of the deposited material. Therefore the blueish colour to 0.4 M NiO thin film is due to nonstoichiometricity. Primarily, when potential is applied, the Ni^{2+} ions start to reduce and formation of nickel hydroxide deposit on the substrate surface (SS). The process can be represented by following electrochemical reaction.



3.1 Structural analysis

Figure 3a shows the XRD pattern of the deposited NiO electrodes after 500 °C temperature annealing. The XRD pattern

of the NiO electrodes obtained by potentiostatic electrochemical deposition method reveals that the diffractogram is of NiO with face-centred cubic phase crystal structure, also known as the bunsenite structure. Diffraction peaks at $2\theta = 44.4^\circ$ and 51.7° are due to the SS. The lattice constant of cubic unit cell is $a = 0.4177$ nm owing to diffraction peaks at 37.28° , 43.37° , 62.90° and 76.33° which can be filled to (1 1 1), (2 0 0), (2 2 0) and (3 1 1) crystal planes, respectively and resembles NiO (JCPDS 47-1049) [39].

The crystallite sizes of the NiO were calculated using Scherrer formula.

$$D = k\lambda/\beta \cos \theta \quad (3)$$

where D , K , λ , β , are crystallite size, Scherrer constant, wavelength of the X-ray radiation (for Cu $K\alpha$, $\lambda = 0.1540$ nm) and full width half maximum (FWHM) of diffraction peak evaluated at 2θ respectively. The crystallite size calculated by using Scherrer formula, for N1 is 2.93 nm and for N4 it is 4.29 nm. As the molarity increases the crystallite size then decreases further to attain its least value of (3.39 nm) at N6 (0.6 M) as shown in Fig. 3b. ϵ (micro strain), δ (dislocation density) and SF (stacking fault) developed in electrodes as a function of deposition molarity were calculated using the Eqs. (4), (5) and (6), respectively [43].

$$\epsilon = \beta \cos \theta/4 \quad (4)$$

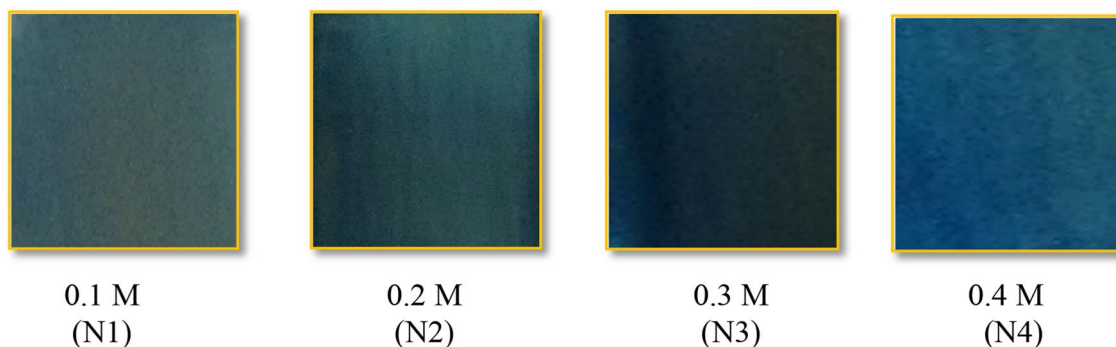
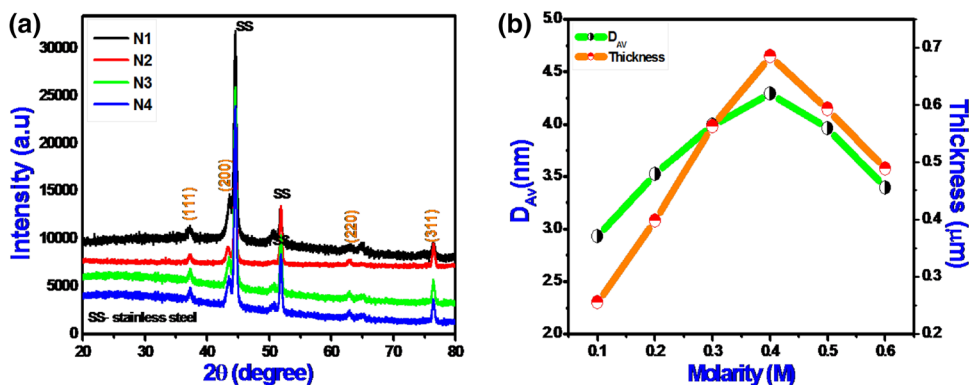


Fig. 2 Photo images of Variation of thin films with different molarities of nickel oxide

Fig. 3 a XRD patterns of NiO film on to stainless steel substrate. b Variation of crystallite size (D_{av}) and thickness (μm) with different molarities of NiO films



$$\delta = 1/D^2 \quad (5)$$

$$SF = [2\pi^2/45(3 \tan \theta)^{1/2}] \beta \quad (6)$$

The effect of various molarities on these parameters is summarized in Table 2. From the table, it is clear that micro strain, dislocation density and stacking fault values are decreased as there is an increase in the crystallite size. The value of micro strain, dislocation density and stacking fault are minute.

3.2 Surface morphology and compositional analyses

Figure 4 displays the SEM micrograph images of NiO films. Figure 4a–d present the micrographs of N1, N2, N3 and N4, respectively. From SEM micrograph, it is evidenced that the exterior part of NiO film is homogenous and of nanoplate-like architecture. To improve electrolyte/electrode junction, this manner of surface promotes to penetrate the electrolyte [44] and such kind of morphology improves the supercapacitive performance of electrode [45]. An EDAX analysis was used to characterize the elemental sharing of the NiO film electrode. The composition of NiO confirms from EDAX data, where individual Ni and O elements are shown

Table 2 Structural parameters ϵ (micro-strain), δ (dislocation density) and SF (stacking fault) were associated with defects

Sr. No	Molarity (M)	D (nm)	Micro strain (ϵ)	Dislocation density (δ)	Stacking fault (SF)
01	N1	2.93	0.1278	0.1164	1.5733
02	N2	3.52	0.1062	0.0807	1.3084
03	N3	3.99	0.0970	0.0628	1.1527
04	N4	4.29	0.0936	0.0543	1.0739

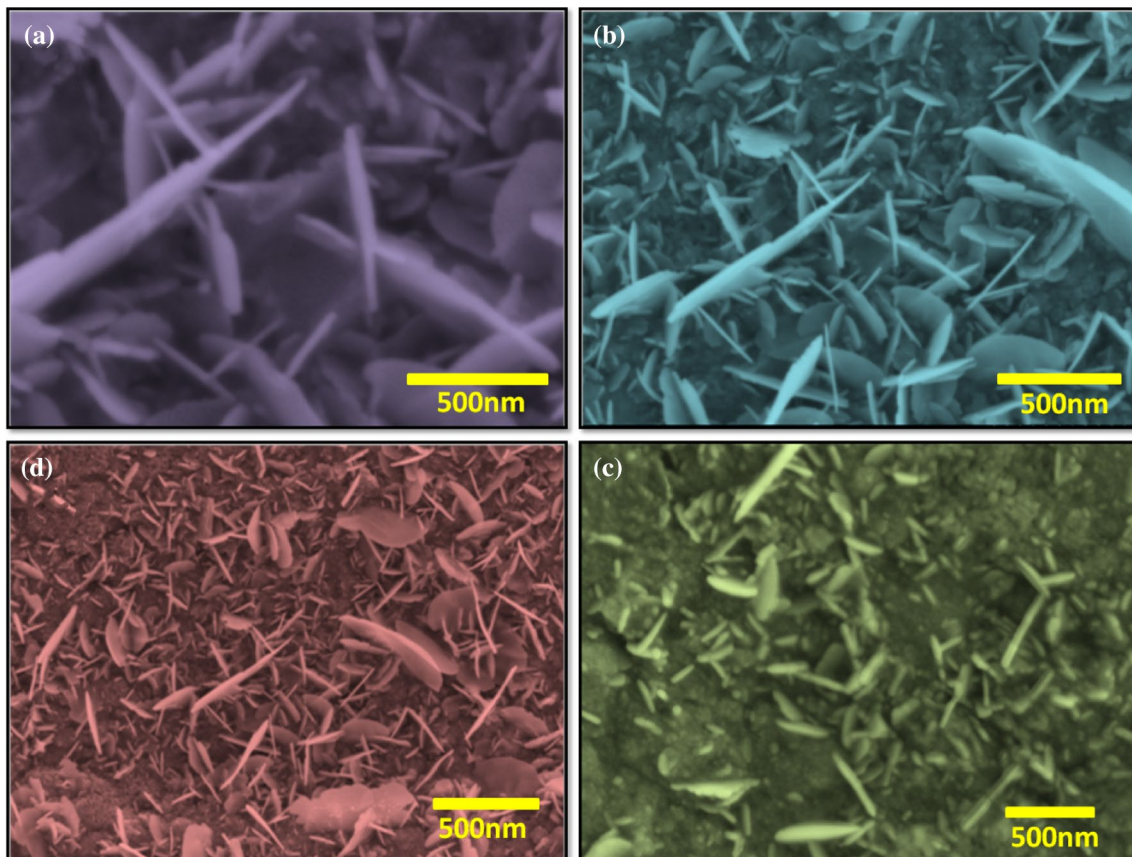


Fig. 4 SEM images of **a** N1, **b** N2, **c** N3 and **d** N4 films

in Fig. 5a–d of N1, N2, N3 and N4 respectively, with their atomic percentages (inset of respective fig). In sample N2, N3 and N4, Fe element peak around 2 keV which is due to stainless steel substrate. It is also seen that as the molarity increases the atomic percentage of nickel is increasing with decrease in atomic percentage of oxygen.

3.3 Surface wettability test

The wetting of water with solid is reliant on the relation among the interfacial tensions (water/air, water/solid and solid/air). The ratio between these tensions decides the contact angle (θ) among a water droplet on a particular surface. A contact angle of 180° corresponds to complete non-wetting and a contact angle of 0° means complete wetting. Both super-hydrophobic and super-hydrophilic surfaces are important for useful applications [46]. While studying supercapacitive properties of the materials, hydrophilicity has more importance. A significant wetting of solid electrode by the electrolyte is only feasible when the surface is hydrophilic in nature. Figure 6a–d show the water contact angle measurement of N1, N2, N3 and N4 film surfaces, respectively. The observed water contact angles are 85° , 88° , 96° and 118° showed the hydrophilic behaviour of N1, N2 thin film ($\theta < 90^\circ$) and hydrophobic behaviour of N3, N4 thin film ($\theta > 90^\circ$). Hydrophilic i.e. high wettability, the strong cohesive force between the water droplet and oxide present in the nickel oxide compound possibly the reason to high wettability. For supercapacitor application, this particular

property is very useful for making close contact of electrode surface with aqueous electrolyte. It is well-known that hydrophilic exterior of the electrode is a chief feature for better performance of the electrochemical capacitors [47].

3.4 X-ray photoelectron spectroscopy analyses

X-ray photoelectron spectroscopy (XPS) technique is used to analyze the chemical state of elements present in NiO nanoplatelets as shown in Fig. 7a. By means of Gaussian curves the Ni 2p spectral peaks in XPS were deconvoluted and the spectrum have two parts characterizing the Ni 2p_{3/2} (850–865 eV) and Ni 2p_{1/2} (870–885 eV) spin–orbit levels. This Ni (2p_{3/2}) and Ni (2p_{1/2}) double peak of Ni (2p), match up to the traced at binding energy of 854.88 and 872.12 eV, respectively as in Fig. 7b, which shows highly determined Ni 2p core level spectrum of NiO. The shake-up satellite peaks were detected at ~ 6.16 and ~ 6.59 eV higher binding energy than that of Ni (2p_{3/2}) and Ni (2p_{1/2}) peaks, respectively. The peak of Ni (2p_{3/2}) at a binding energy of 854.01 eV with their associate shake-up satellite peaks at 860.17 eV showed the presence of Ni²⁺ cations and not of Ni³⁺ cations and the same is observed for Ni (2p_{1/2}) peak also. This observation confirmed the NiO nanoplatelet compiled of pure NiO phase [48, 49]. Particularly, the absence of multiplet splitting of the peaks at 854.01 eV, which corresponds to the oxidation state of Ni²⁺ corroborates the formation of NiO only rather than any other oxidation states of nickel. The Ni (2p_{3/2}) and Ni (2p_{1/2}) peaks are separated

Fig. 5 EDAX of **a** N1, **b** N2, **c** N3 and **d** N4 films

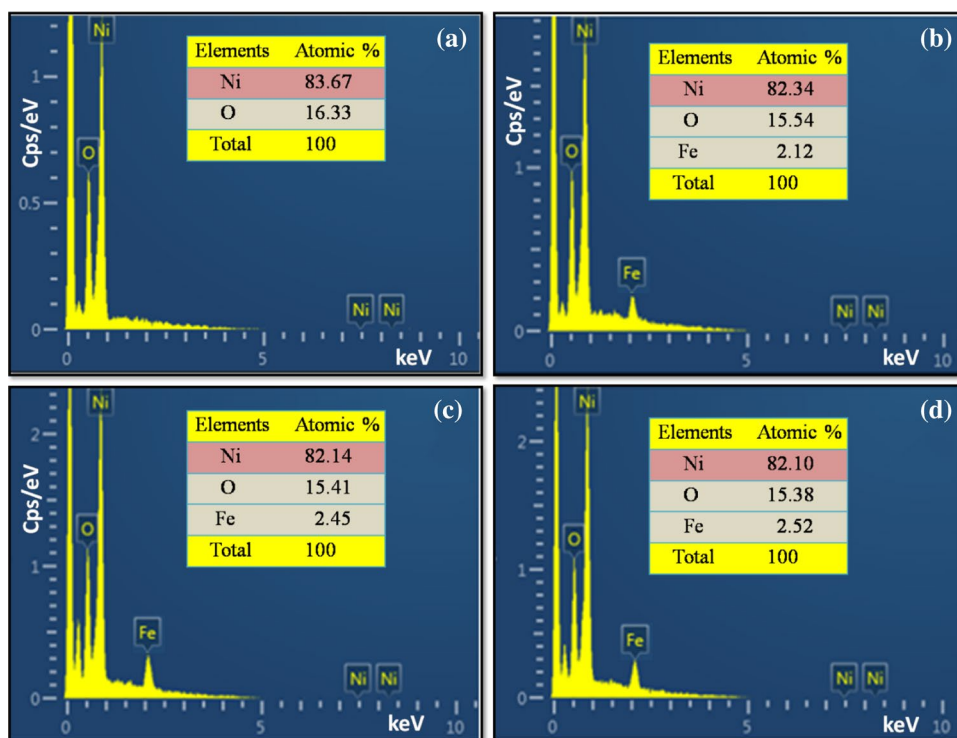


Fig. 6 The water contact angle measurement images of **a** N1, **b** N2, **c** N3 and **d** N4 films

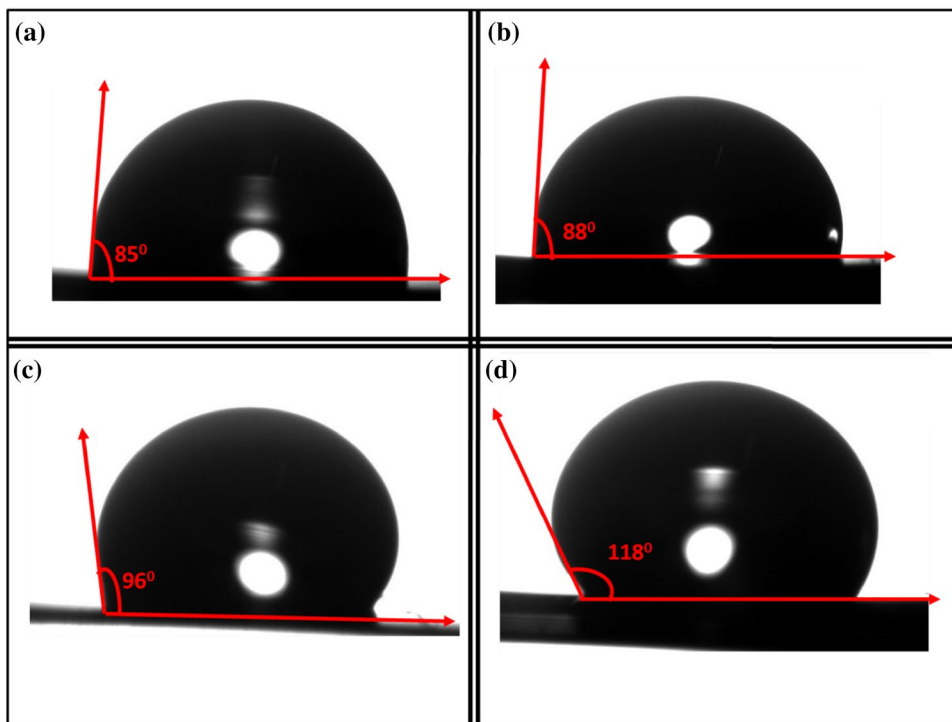
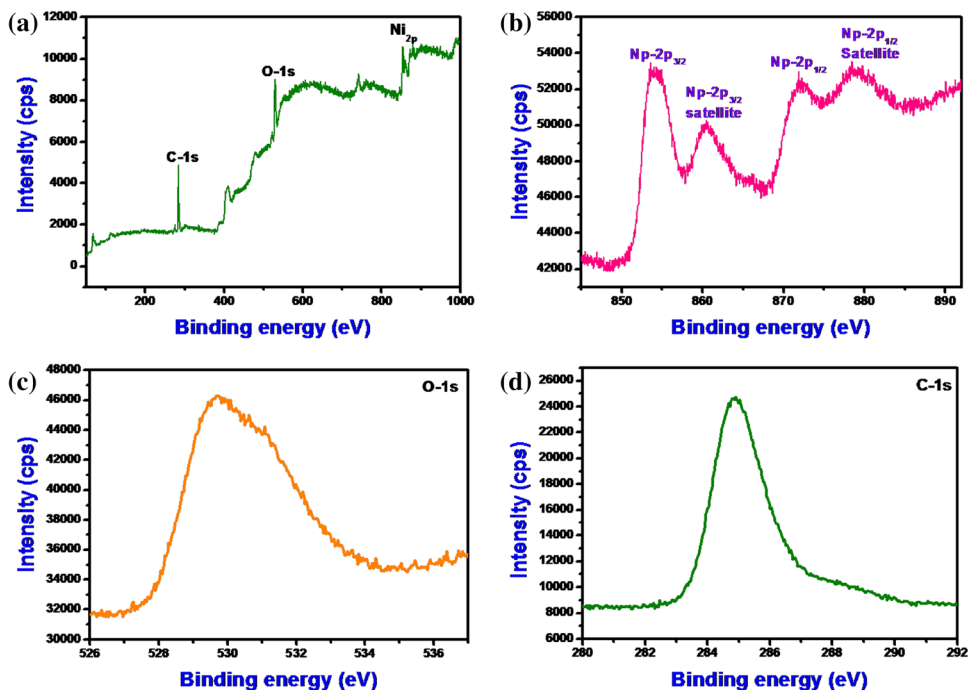


Fig. 7 **a** Survey XPS spectrum of NiO nanoplatelets grown on SS substrate, **b** Ni 2p core-level spectrum, **c** O1s spectrum and **d** C1s spectrum



by 17.24 eV, which also confirms the formation of only NiO rather than any other phase of nickel oxide [50].

Figure 7c, d shows the spectra of O1s and C1s respectively, also hold the characteristic peaks detected in Ni2p spectrum. The peak at 529.69 eV in O1s matches to the

O-1 s core level of the O²⁻ anions in the NiO. In the C-1 s spectrum of carbon, the peaks characterize the existence of atmospheric carbon, which is very probable and indeed, it is frequently used to standardize peak positions.

3.5 Electrochemical supercapacitive measurements

The electrodeposited NiO electrodes with different molarities (N1, N2, N3 and N4) were tested using CV measurement for supercapacitive performance. For all NiO electrodes, the C (capacitance) was calculated using following relation;

$$C = I/(dV/dt) \quad (7)$$

where I (current) in Ampere and dV/dt (voltage scanning rate) of NiO electrode dipped in electrolyte. For all NiO electrodes, the C_i (interfacial capacitance) was calculated using the relation;

$$C_i = C/A \quad (8)$$

where 'A' (area of active material dipped in the electrolyte).

For all NiO electrodes, the SC (specific capacitance) was calculated using following relation;

$$SC = C/W \quad (9)$$

where W (mass) of nickel oxide on surface of SS dipped in electrolyte.

3.6 Cyclic voltammogram analysis

3.6.1 Effect of variation of nickel oxide film electrodes with different molarities and scan rate

In the field of electrochemistry, CV is a dominant tool for primary screening of materials when used in electrochemical capacitors. It has been utilized broadly to characterize the performance of different energy storage devices. With an aim to know the supercapacitive performance of NiO film electrode, CV curves were recorded in a potential range -1.2 and 1.2 V in 1 M Na_2SO_4 . Accordingly, a relative study of CV plots of NiO electrodes i.e. N1 to N4 are shown in Fig. 8a–d respectively at different scanning rates and N1 to N4 single curves at 25 mV/s scan rate shown in Fig. 8e. In this work, nanostructured NiO with average particle sizes of 2.93 , 3.52 , 3.99 and 4.29 nm were synthesized via potentiostatic electrochemical deposition method. The NiO with different particle sizes were evidently explored for electrochemical performance. From Table 3 it is clear that, with increase in the molarity of NiO the SC is decreased. Surface area to volume ratio is inversely proportional to size and surface area is directly proportional to capacitance so we believe that this is caused by crystallite size. For N1, crystallite size is lowest and for N4 it is highest, so for further analysis we utilized N1 electrode only.

3.6.2 Effect of various electrolytes and scan rate

The electrochemical properties of the supercapacitors based on electrodeposited N1 electrode was investigated by CV measured in 1 M aqueous Na_2SO_4 , NaOH and KOH electrolytes in potential range -1.2 to $+1.2$ V, -1.2 to $+0.4$ V and $+0.2$ to $+0.4$ V, respectively versus reference electrode i.e. SCE. The aqueous electrolytes were selected because of: it demonstrates superior power and higher concentration than those with organic electrolytes, possibly due to higher ionic concentration and smaller ionic radius [51]. Figure 9 displays CV curves of N1 electrode in different electrolytes such as Na_2SO_4 , NaOH and KOH . The SC values in different electrolytes are calculated by using Eq. (9), also specific energy (Whkg^{-1}), specific power (kWkg^{-1}) and coulombic efficiency (%) were calculated using Eqs. (10), (11) and (12), respectively. The Na_2SO_4 electrolyte is the most considerable electrolyte judged to others apparent from Table 4, because it gives highest SC value compared to NaOH and KOH electrolytes as well as its specific energy, specific power and coulombic efficiency is also finer than the others.

3.6.3 Effect of electrolyte concentration and scan rate

In the current investigation, we further have investigated the effect of optimized electrolyte concentration on electrochemical supercapacitor performance. The electrochemical supercapacitive properties such as CV study of N1 electrode investigated at 0.25 , 0.50 and 1 M concentrations of Na_2SO_4 aqueous electrolyte is shown in Fig. 10. Table 5 shows the variation of SC value with molarity of Na_2SO_4 in electrolyte solution for N1 electrode. A maximum value of 667.24 Fg^{-1} was obtained for 1 M solution molarity of Na_2SO_4 at 5 mV/s scan rate. This value is better than those of other metal oxides such as MnO_2 , Co_3O_4 [52, 53]. The influence of the precursor molarity of Na_2SO_4 in electrolyte solution within the nickel oxide electrode on the CV analysis is apparent. In the present investigation, high specific capacitance (667.24 Fg^{-1}) may be attributed to the high surface area and homogenous structure of N1 electrode as observed from SEM, which can be beneficial for intercalation/deintercalation of ions. Figure 11a shows typical CV plots of N1 electrode in 1 M Na_2SO_4 electrolyte at 5 , 25 , 50 , 75 and 100 mV/s scan rates. The area under the curve is increased with scan rate. It means that the CV area is directly proportional to the scan rate, indicating capacitive behaviour of N1 electrode [54]. Figure 11b shows variation of specific and interfacial capacitances at different scan rates. From figure, it is seen that both values are decreased from 667.24 to 151.44 Fg^{-1} and 0.66 to 0.36 Fcm^{-2} , respectively.

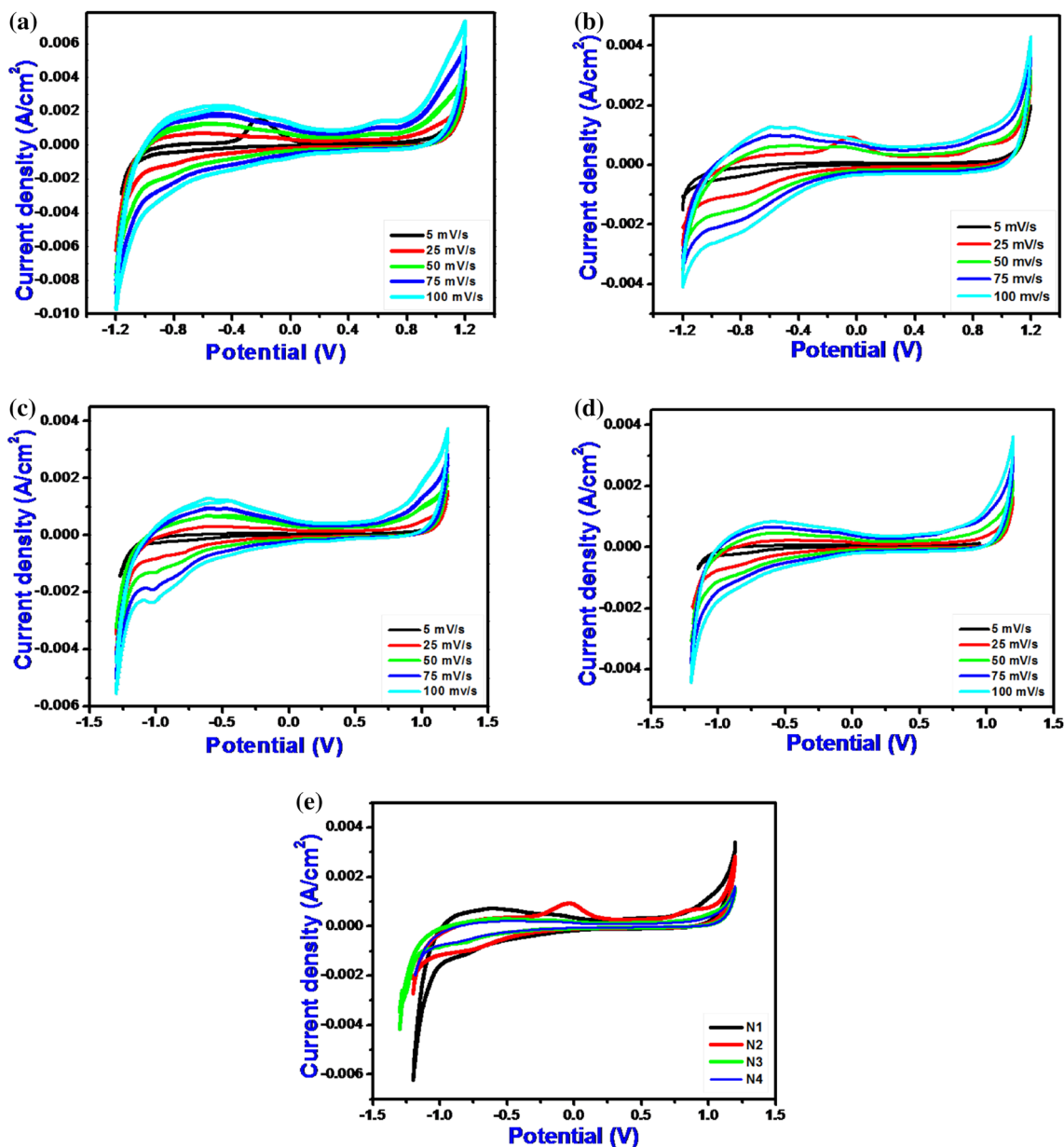


Fig. 8 Cyclic voltammogram of nickel oxide electrodes a N1, b N2, c N3, d N4 at different scanning rates and e N1 to N4 at 25 mV/s scan rate

Table 3 Different molarities in 1 M Na₂SO₄ electrolyte with 5 mV/s scan rate data

Sr. No	Molarity	D _{AV} (nm)	SC (Fg ⁻¹)
01	N1	2.93	667.24
02	N2	3.52	327.81
03	N3	3.99	252.17
04	N4	4.29	114.87

3.7 Galvanometric charge–discharge studies

A galvanostatic charge–discharge test is conducted in a stable potential window at current density of 1 mA g⁻¹, for N1 electrode and the result are shown in Fig. 11c. The N1 electrode has exhibited a non-linear charge–discharge profile, which diverges from the classic linear variation of voltage with time, usually demonstrated by an electrochemical double layer capacitor, can be described as due to the redox reaction occurring at this voltage range. This also replies an insignificant ohmic drop. During the charging process, the potential rapidly elevates up to designated value caused by

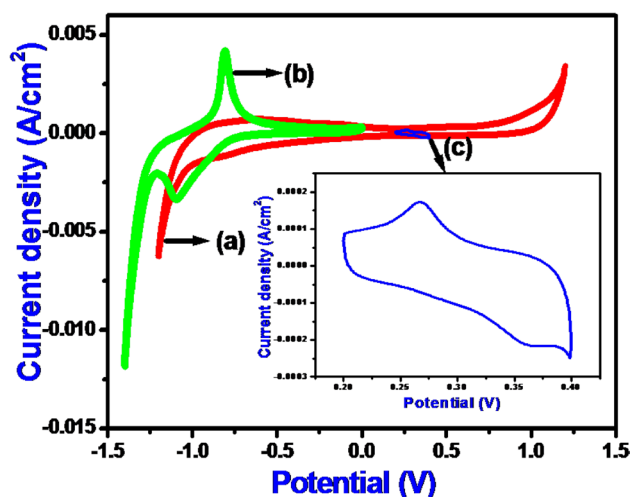


Fig. 9 Cyclic voltammograms of N1 electrode in 1 M **a** Na₂SO₄, **b** NaOH, **c** KOH electrolytes

the oxidation of NiO. While, in the discharging process the electrode potential reduces sharply due to the internal resistance (IR) followed by a slow decline [55]. Charge–discharge curves point out a good capacitive performance of N1 electrode [17]. The electrochemical parameters for example, specific energy (E), specific power (P) and coulomb efficiency (η) are calculated using following relations.

$$E = (V \times I_d \times T_d) / W \quad (10)$$

$$P = (V \times I_d) / W \quad (11)$$

$$\eta \% = (t_d / t_c) \times 100 \quad (12)$$

where V (applied potential), W (mass) of NiO film electrode. t_c , t_d and I_d are charge time, discharge time and discharge current, respectively. The maximal values of E (specific energy), P (specific power) and η (coulombic efficiency) values are 2.55 Whkg⁻¹, 6.23 kWkg⁻¹ and 92.86% respectively at current density 1 mAcm⁻² for N1 electrode.

3.8 Electrochemical impedance analyses

The EIS measurement was used to study of nickel oxide N1 electrode and in addition charge transfer steps at the N1 electrode/Na₂SO₄ electrolyte interface in quantitative manner.

Figure 11d shows the relevant Nyquist plot of supercapacitor cell assembly based on the high surface area N1 electrode in the aqueous solution of 1 M Na₂SO₄ using a three-electrode system in the frequency range of 0.1 Hz–1 MHz. From figure it is seen that, the cell has a semicircle in the high frequency segment and afterwards illustrates a straight line in the low frequency segment. Inset of Fig. 11d shows enlarged piece of semicircle in the high frequency section. Inset of Fig. 11d displays the equivalent circuit fitted to impedance data. Equivalent series resistance (ESR) is 0.1 Ω which is combination of ionic resistance, intrinsic resistance and contact resistance [56]. A semicircle in the higher frequency region involves the parallel combination $R2$ (charge transfer resistance) caused by the Faradic reactions and the constant phase element (CPE) consequence of nonuniform distribution due to inhomogeneous charge accumulation at electrode exterior and W is the Warburg impedance due to diffusion of Na⁺ in electrode [57]. In the present study, the values of equivalent series resistance and charge transfer resistance were considerably lower which lead to greater values of supercapacitive parameters. Figure 11e shows the electrochemical stability of N1 electrode reveals decrease of SC value with increase in cycle numbers. After 1000th cycles the capacitance retention ratio of the N1 electrode was 90.7%, which imply an

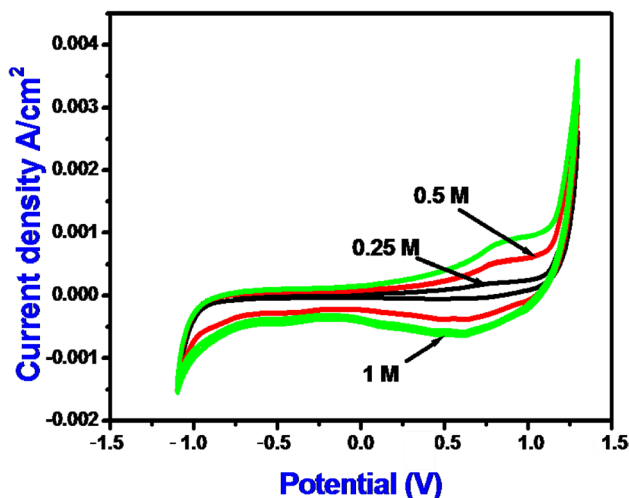


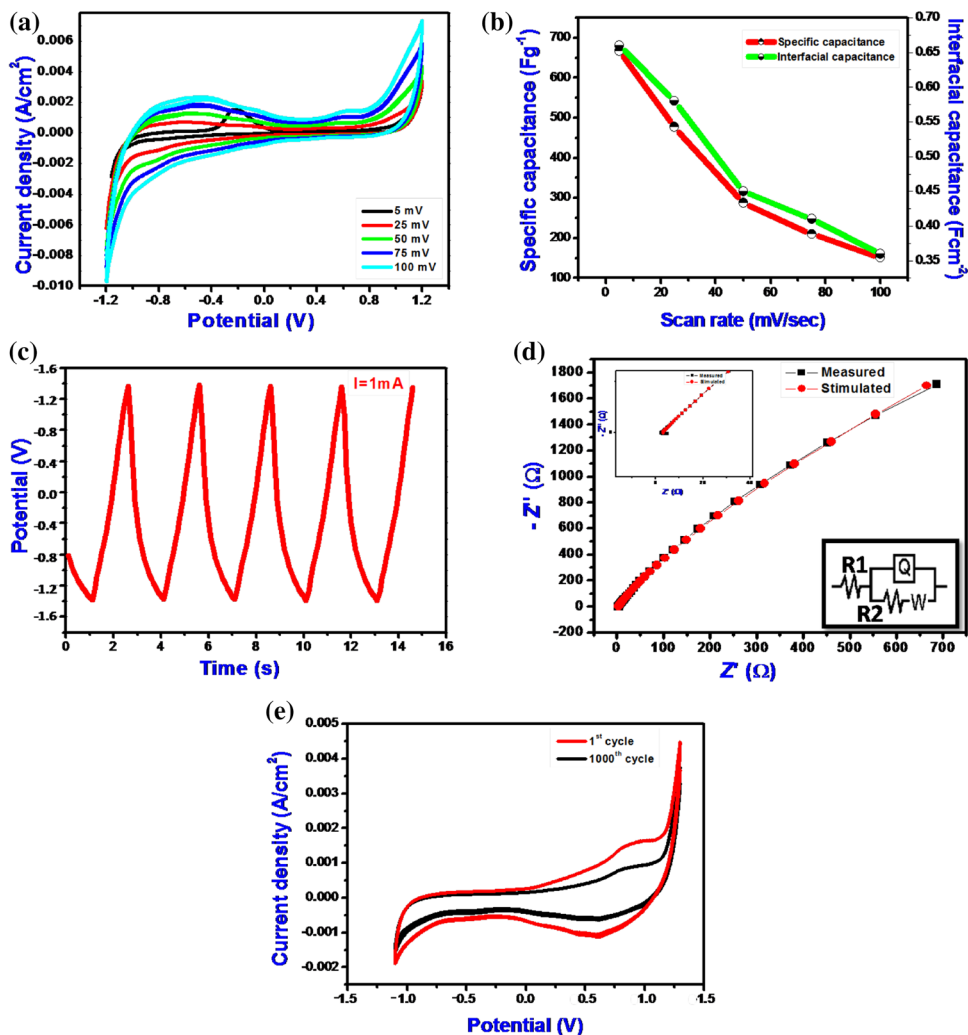
Fig. 10 Cyclic voltammograms of N1 electrode in **a** 1 M, **b** 0.5 M, **c** 0.25 M of Na₂SO₄ electrolyte

Table 4 Various electrolytes of 1 M with 5 mV/s scan rate data

Sr. No	Electrolyte	Specific energy (Whkg ⁻¹)	Specific power (kWkg ⁻¹)	Coulomb efficiency (η %)	Specific capacitance (Fg ⁻¹)
01	Na ₂ SO ₄	2.55	6.23	99.94	667.24
02	NaOH	0.13	0.62	97.86	278.44
03	KOH	0.38	1.74	88.86	135.31

Table 5 Variation of 1 M Na₂SO₄ electrolyte concentration with 5 mV/s scan rate data

Sr. No	Na ₂ SO ₄ concentration (M)	Specific energy (Whkg ⁻¹)	Specific power (kWkg ⁻¹)	Coulomb efficiency (η %)	Specific capacitance (Fg ⁻¹)
01	0.25	0.21	0.72	89.96	164.57
02	0.5	0.66	1.86	92.88	204.33
03	1	2.55	6.23	99.94	667.24

Fig. 11 **a** Cyclic voltammogram of N1 electrode at different scanning rate. **b** Variation of specific and interfacial capacitances at different scan rates. **c** The charge–discharge curve of N1 electrode in 1 M Na₂SO₄ electrolyte. **d** Nyquist plot obtained for N1 electrode in 1 M Na₂SO₄ electrolyte. **e** Stability study of N1 electrode

outstanding long-term recycling potential of NiO electrode than the values reported by Duraisamy et al. [38].

4 Conclusions

For the deposition of NiO films with various concentrations the potentiostatic electrochemical deposition method has been effectively employed. The XRD, EDAX and XPS measurements evidence for the NiO whereas, SEM measurement shows homogenous and smooth morphology

which is suitable for supercapacitors. The NiO electrode has revealed the excellent performance with the maximum value of specific capacitance of 667.24 Fg⁻¹ when used in electrochemical measurement in 1 M Na₂SO₄ electrolyte. The charge–discharge study predicts the high power capability of the NiO electrode with significant value of energy. The maximum values of specific energy, specific power and coulomb efficiency are 2.55 Whkg⁻¹ and 6.23 kWkg⁻¹ and 92.86%, respectively. An electrochemical impedance spectroscopy study demonstrated beneficial for an electrode in supercapacitors.

Acknowledgements Prof. V.B. Patil is thankful to the CSIR (India), for financial support through Scheme No. 03 (1319)/14/EMR-II. Authors also would like to thank DAE-BRNS for the financial support through Scheme No. 34/14/21/2015-BRNS and RUSA Maharashtra for the financial support through Scheme No. RUSA/R&I/2016/267.

References

- J.R. Miller, A.F. Burke, Electrochemical capacitors: challenges and opportunities for real-world applications. *Electrochem. Soc. Interface* **17**, 53 (2008)
- S.M. Ingole et al., An approach to harness energy by SnO₂ thin film electrode by thermal evaporation, in *Techno-Societal 2016. ICATSA 2016*, ed. by P. Pawar, B. Ronge, R. Balasubramaniam, S. Seshabhatter (Springer, Cham, 2018)
- P.J. Hall, M. Mirzaeian, S.I. Fletcher, F.B. Sillars, A.J.R. Rennie, G.O. Shitta-bey, G. Wilson, A. Cruden, R. Carter, Energy storage in electrochemical capacitors: designing functional materials to improve performance. *Energy Environ. Sci.* **3**, 1238 (2010)
- Z. Chen, W. Ren, L. Gao, B. Liu, S. Pei, H.M. Cheng, Three-dimensional flexible and conductive interconnected graphene networks grown by chemical vapour deposition. *Nat. Mater.* **10**, 424 (2011)
- P.C. Chen, G. Shen, G. Shi, H. Chen, C. Zhou, Preparation and characterization of flexible asymmetric supercapacitors based on transition-metal-oxide nanowire/single-walled carbon nanotube hybrid thin film electrodes. *ACS Nano* **4**, 4403 (2010)
- K. Krishnamoorthy, G. Veerasubramani, S. Radhakrishnan, S.J. Kim, One pot hydrothermal growth of hierarchical nanostructured Ni₃S₂ on Ni foam for supercapacitor application. *Chem. Eng. J.* **251**, 116 (2014)
- A. Ramadoss, S.J. Kim, Improved activity of a graphene–TiO₂ hybrid electrode in an electrochemical supercapacitor. *Carbon* **63**, 434 (2013)
- I.A. Dhole et al., Efficient electrodeposited nickel oxide thin films for supercapacitor electrode, in *Techno-Societal 2016. ICATSA 2016*, ed. by P. Pawar, B. Ronge, R. Balasubramaniam, S. Seshabhatter (Springer, Cham, 2018)
- M. Liu, J. Chang, J. Sun, L. Gao, Synthesis of porous NiO using NaBH₄ dissolved in ethylene glycol as precipitant for high-performance supercapacitor. *Electrochim. Acta* **107**, 9 (2013)
- S.K. Meher, P. Justin, G.R. Rao, Microwave-mediated synthesis for improved morphology and pseudocapacitance performance of nickel oxide. *ACS Appl. Mater. Interfaces* **3**, 2063 (2011)
- S.M. Ingole, S.T. Navale, Y.H. Navale, I.A. Dhole, R.S. Mane, F.J. Stadler, V.B. Patil, Galvanostatically electroplated MnO₂ nanoplate-type electrode for potential electrochemical pseudocapacitor application. *J. Solid State Electrochem.* **21**, 1817 (2017)
- P.D. More, P.R. Jadhav, A.A. Ghanwat, I.A. Dhole, Y.H. Navale, V.B. Patil, Spray synthesized hydrophobic α -Fe₂O₃ thin film electrodes for supercapacitor application. *J. Mater. Sci.* **28**, 17839 (2017)
- W. Deng, Y. Liu, Y. Zhang, F. Lu, Q. Chen, X. Ji, Enhanced electrochemical capacitance of nanoporous NiO based on an eggshell membrane. *RSC Adv.* **2**, 1743 (2012)
- S.I. Kim, J.S. Lee, H.J. Ahn, H.K. Song, J.H. Jang, Facile route to an efficient NiO supercapacitor with a three-dimensional nanonetwork morphology. *ACS Appl. Mater. Interfaces* **5**, 1596 (2013)
- C.Z. Yuan, X.G. Zhang, L.H. Su, B. Gao, L.F. Shen, Facile synthesis and self-assembly of hierarchical porous NiO nano/micro spherical superstructures for high performance supercapacitors. *J. Mater. Chem.* **19**, 5772 (2009)
- J.W. Lang, L.B. Kong, W.J. Wu, Y.C. Luo, L. Kang, Facile approach to prepare loose-packed NiO nano-flakes materials for supercapacitors. *Chem. Commun.* **35**, 4213 (2008)
- M.S. Wu, M.J. Wang, Nickel oxide film with open macropores fabricated by surfactant-assisted anodic deposition for high capacitance supercapacitors. *Chem. Commun.* **46**, 6968 (2010)
- H. Wang, H. Yi, X. Chen, X. Wang, Facile synthesis of a nanostructured nickel oxide electrode with outstanding pseudocapacitive properties. *Electrochim. Acta* **105**, 353 (2013)
- Q. Li, L.S. Wang, B.Y. Hu, C. Yang, L. Zhou, L. Zhang, Preparation and characterization of NiO nanoparticles through calcination of malate gel. *Mater. Lett.* **61**, 1615 (2007)
- A. Aslani, V. Oroojpour, M. Fallahi, Sonochemical synthesis, size controlling and gas sensing properties of NiO nanoparticles. *Appl. Surf. Sci.* **257**, 4056 (2011)
- F. Davar, Z. Fereshteh, M. Salavati-Niasari, Nanoparticles Ni and NiO: synthesis, characterization and magnetic properties. *J. Alloys Compd.* **476**, 797 (2009)
- I.A. Dhole, S.T. Navale, Y.H. Navale, Y.M. Jadhav, C.S. Pawar, S.S. Suryavanshi, V.B. Patil, Performance evaluation of galvanostatically deposited nickel oxide electrode for electrochemical supercapacitors. *J. Mater. Sci.* **28**, 10819 (2017)
- V.V. Kondalkar, S.S. Yang, P.S. Patil, S. Choudhury, P.N. Bhosale, K.K. Lee, Langmuir-Blodgett assembly of nanometric WO₃ thin film for electrochromic performance: a new way. *Mater. Lett.* **194**, 102 (2017)
- Y. Zhang, J. Li, F. Kang, F. Gao, X. Wang, Fabrication and electrochemical characterization of two-dimensional ordered nanoporous manganese oxide for supercapacitor applications. *Int. J. Hydrog. Energy* **37**, 860 (2012)
- V.V. Kondalkar, P.B. Patil, R.M. Mane, P.S. Patil, S. Choudhury, P.N. Bhosale, Electrochromic performance of nickel oxide thin film: synthesis via electrodeposition technique. *Macromol. Symp.* **361**, 47 (2016)
- S.T. Navale, V.V. Mali, S.A. Pawar, R.S. Mane, M. Naushad, F.J. Stadler, V.B. Patil, Electrochemical supercapacitor development based on electrodeposited nickel oxide film. *RSC Adv.* **5**, 51961 (2015)
- V.V. Kondalkar, R.R. Kharade, S.S. Mali, R.M. Mane, P.B. Patil, P.S. Patil, S. Choudhury, P.N. Bhosale, Nanobrick-like WO₃ thin films: hydrothermal synthesis and electrochromic application. *Superlattices Microstruct.* **73**, 290 (2014)
- V.V. Kondalkar, S.S. Mali, R.R. Kharade, R.M. Mane, P.S. Patil, C.K. Hong, J.H. Kim, S. Choudhury, P.N. Bhosale, Langmuir-Blodgett self organized nanocrystalline tungsten oxide thin films for electrochromic performance. *RSC Adv.* **24**, 26923 (2015)
- J. Zhu, J. Jiang, J. Liu, R. Ding, H. Ding, Y. Feng, G. Wei, X. Huang, Direct synthesis of porous NiO nanowall arrays on conductive substrates for supercapacitor application. *J. Solid State Chem.* **184**, 578 (2011)
- Y. Wang, Y. Xia., Electrochemical capacitance characterization of NiO with ordered mesoporous structure synthesized by template SBA-15. *Electrochim. Acta* **51**, 3223 (2006)
- B. Ren, M. Fan, Q. Liu, J. Wang, D. Song, X. Bai, Hollow NiO nanofibers modified by citric acid and the performances as supercapacitor electrode. *Electrochim. Acta* **92**, 197 (2013)
- A.I. Inamdar, Y.S. Kim, S.M. Pawar, J.H. Kim, H. Im, H. Kim, Chemically grown, porous, nickel oxide thin-film for electrochemical supercapacitors. *J. Power Sources* **196**, 2393 (2011)
- C.Y. Cao, W. Guo, Z.M. Cui, W.G. Song, W. Cai, Microwave-assisted gas/liquid interfacial synthesis of flowerlike NiO hollow nanosphere precursors and their application as supercapacitor electrodes. *J. Mater. Chem.* **21**, 3204 (2011)
- S. Ding, T. Zhu, J.S. Chen, Z. Wang, C. Yuan, X.W. Lou, Controlled synthesis of hierarchical NiO nanosheet hollow spheres

- with enhanced supercapacitive performance. *J. Mater. Chem.* **21**, 6602 (2011)
35. U.M. Patil, R.R. Salunkhe, K.V. Gurav, C.D. Lokhande, Chemically deposited nanocrystalline NiO thin films for supercapacitor application. *Appl. Surf. Sci.* **255**, 2603 (2008)
 36. M.S. Wu, M.J. Wang, J.J. Jow, Fabrication of porous nickel oxide film with open macropores by electrophoresis and electrodeposition for electrochemical capacitors. *J. Power Sources* **195**, 3950 (2010)
 37. H.M. Shiri, M. Aghazadeh, Synthesis, characterization and electrochemical properties of capsule-like NiO nanoparticles. *J. Electrochem. Soc.* **159**, E132 (2012)
 38. N. Duraisamy, A. Numan, S.O. Fatin, K. Ramesh, S. Ramesh, Facile sonochemical synthesis of nanostructured NiO with different particle sizes and its electrochemical properties for supercapacitor application. *J. Colloid Interface Sci.* **471**, 136 (2016)
 39. M.S. Wu, Y.A. Huang, C.H. Yang, J.J. Jow, Electrodeposition of nanoporous nickel oxide film for electrochemical capacitors. *Int. J. Hydrog. Energy* **32**, 4153 (2007)
 40. A.D. Jagadale, V.S. Kumbhar, D.S. Dhawale, C.D. Lokhande, Potentiodynamically deposited nickel oxide (NiO) nanoflakes for pseudocapacitors. *J. Electroanal. Chem.* **704**, 90 (2013)
 41. M.S. Wu, C.Y. Huang, K.H. Lin, Electrophoretic deposition of nickel oxide electrode for high-rate electrochemical capacitors. *J. Power Sources* **186**, 557 (2009)
 42. A.D. Jagadale, D.P. Dubal, C.D. Lokhande, Electrochemical behavior of potentiodynamically deposited cobalt oxyhydroxide (CoOOH) thin films for supercapacitor application. *Mater. Res. Bull.* **47**, 672 (2012)
 43. V.V. Kondalkar, S.S. Mali, N.B. Pawar, R.M. Mane, S. Choudhury, C.K. Hong, P.S. Patil, S.R. Patil, P.N. Bhosale, J.H. Kim, Microwave-assisted rapid synthesis of highly porous TiO₂ thin films with nanocrystalline framework for efficient photoelectrochemical conversion. *Electrochim. Acta* **143**, 89 (2014)
 44. S.B. Jambure, C.D. Lokhande, Photoelectrochemical solar cells with chemically grown CdO rice grains on flexible stainless steel substrates. *Mater. Lett.* **106**, 133 (2013)
 45. C. Ye, Z.M. Lin, S.Z. Hui, Electrochemical and capacitance properties of rod-shaped MnO₂ for supercapacitor. *J. Electrochem. Soc.* **152**, A1272 (2005)
 46. R.D. Sun, A. Nakajima, A. Fujushima, T. Watanabe, K. Hashimoto, Photoinduced surface wettability conversion of ZnO and TiO₂ thin films. *J. Phys. Chem. B* **105**, 1984 (2001)
 47. O. Bockman, T. Ostvold, G.A. Voyiatzis, G.N. Papatheodorou, Raman spectroscopy of cemented cobalt on zinc substrates. *Hydrometallurgy* **55**, 93 (2000)
 48. X. Zhang, W. Shi, J. Zhu, W. Zhao, J. Ma, S. Mhaisalkar, T.L. Maria, Y. Yang, H. Zhang, H.H. Hng, Q. Yan, Synthesis of porous NiO nanocrystals with controllable surface area and their application as supercapacitor electrodes. *Nano Research* **3**, 643 (2010)
 49. A.P. Grosvenor, M.C. Biesinger, R.S.C. Smart, N.S. McIntyre, New interpretations of XPS spectra of nickel metal and oxides. *Surf. Sci.* **600**, 1771 (2006)
 50. M.C. Biesinger, B.P. Payne, L.W.M. Lau, A. Gerson, R.S.C. Smart, X-ray photoelectron spectroscopic chemical state quantification of mixed nickel metal, oxide and hydroxide system. *Surf. Interface Anal.* **41**, 324 (2009)
 51. P.D. More, P.R. Jadhav, S.M. Ingole, Y.H. Navale, V.B. Patil, Preparation, structural and electrochemical supercapacitive properties of sprayed manganese oxide film electrode. *J. Mater. Sci.* **28**, 707 (2017)
 52. D.P. Dubal, D.S. Dhawale, T.P. Gujar, C.D. Lokhande, Effect of different modes of electrodeposition on supercapacitive properties of MnO₂ thin films. *Appl. Surf. Sci.* **257**, 3378 (2011)
 53. A.D. Jagadale, V.S. Kumbhar, R.N. Bulakhe, C.D. Lokhande, Influence of electrodeposition modes on the supercapacitive performance of Co₃O₄ electrodes. *Energy* **64**, 234 (2014)
 54. Y.H. Navale, S.M. Ingole, S.T. Navale, F.J. Stadler, R.S. Mane, V.B. Mu. Naushad, Patil, Electrochemical synthesis and potential electrochemical energy storage performance of nodule-type polyaniline. *J. Colloid Interface Sci.* **487**, 458 (2017)
 55. W.G. Pell, B.E. Conway, Analysis of power limitations at porous supercapacitor electrodes under cyclic voltammetry modulation and dc charge. *J. Power Sources* **96**, 57 (2001)
 56. J. Gamby, P.L. Taberna, P. Simon, J.F. Fauvarque, M. Chesneau, Studies and characterisations of various activated carbons used for carbon/carbon supercapacitors. *J. Power Sources* **101**, 109 (2001)
 57. S.C. Pang, B.H. Wee, S.F. Chin, The capacitive behaviors of manganese dioxide thin-film electrochemical capacitor prototypes. *Int. J. Electrochem.* **2011**, 1 (2011)